Iranian Journal of Mechanical Engineering
The Iranian Society of Mechanical Engineers
Research Paper
DOI: 10.30506/jmee.2021.131971.1239

A Shell Superelement for Mechanical Analysis of Cylindrical Structures

A. Jafarzadeh*
M.Sc.

A. Taghvaeipour†
Assistant Profesore

M. R. Eslami ‡
Professor

This paper aims at developing a new cylindrical shell element, called shell superelement. The element is defined based on the classical shell theory, and it consists of eight nodes each with six degree-of-freedoms (dofs). In this element, the trigonometric shape functions are incorporated along the angular direction of element while polynomials were used in other two directions. Therefore, there is no need for meshing a shell structure with cylindrical geometry through the angular direction. This property helps an engineer to deal with complicated analyses on cylindrical shell structures with less number of dofs. At the end, the defined element is used in the stress analysis of two different classical shell problems and the results are compared with the ones reported in the literature, and obtained by means of shell elements in a commercial software package.

Keywords: Cylindrical Shell element, Superelement, Trigonometric shape functions, Structural analysis

1 Introduction

At the embodiment stage of design, engineers and researchers usually conduct rigorous analyses on a target component or structure. This can be obtained via analytical or numerical methods. In analytical methods, the governing equations of a component are solved by mathematical approaches such as Fourier series, Laplace transform and etc. However, in numerical methods the governing equations are handled with numerical calculations such as finite element method, finite difference method, generalized differential quadrature and etc. With the recent development of numerical algorithms and computer processors, numerical methods can efficiently solve complicated problems. As a result, several software packages are now available in a variety of engineering fields. The finite element method is one of the important numerical approaches which is commonly used in modeling and analysis of complex structures. In this method, a structure is discretized into many elements in which mathematical functions, so called *shape functions*, approximate a physical variable such as displacement or temperature

* M.Sc., Mechanical Engineering, Department of Mechanical Engineering, Amirkabir University of Technology, Tehran, Iran Jafarzadeh-Ayat@aut.ac.ir
† Corresponding Author, Assistant Professor, Mechanical Engineering, Department of Mechanical Engineering, Amirkabir University of Technology, Tehran, Iran ataghvaei@aut.ac.ir
‡ Professor and Fellow of the Academy of Sciences, Mechanical Engineering, Department of Mechanical Engineering, Amirkabir University of Technology, Tehran, Iran Eslami@aut.ac.ir
Receive : 2020/08/01 Accepted : 2021/01/18

within the elements. Due to simplicity, basic geometries such as hexahedron or tetrahedron elements are commonly used to discretize a structure. Moreover, with these basic geometries, the physical variables are commonly approximated by means of polynomial shape functions. Although this combination is proved to be very efficient in analysis of components with complex geometry, its accuracy mostly relies on the quality of discretization, which normally depends on the number of elements. Recently, researchers proposed new elements with more complex shape functions and geometries, which are defined for components with specific geometries. These elements are called *superelements* [1]. Accordingly, a component can be analyzed with a limited number of such elements, which leads to a significant reduction of computational cost. In this regard, Koko and Olson first used the super plate and beam finite elements to calculate the natural frequency and modal shapes of stiffened rectangular plates. They validated the results with other numerical and experimental works [2]. Jiang and Olson [3, 4], introduced shell, curved beam, and straight beam superelements for the free vibration analysis of stiffened cylindrical shells. The foregoing superelements were further applied to analyze the static and dynamic behavior of orthogonally stiffened cylindrical shells. The stiffeners were also assumed to be in form of curved and straight beams. In addition, the results, including the natural frequencies and mode shapes, were compared with the conventional finite element method and experimental tests. The authors reported high rate of convergence and accuracy comparing with the results of other methods. Ahmadian et al. [5, 6] employed the plate superelement to analyze the forced and free vibrations of an orthotropic rectangular plate with different boundary conditions. They considered bending and in-plane effects on the response of the plate; they also assumed C^0-continuity for in-plane displacements and C^1-continuity for out of plane displacements. Kuntjoro et al. [7] conducted a stress and deflection analysis on a Figurehter wing structure by means of superelements. However, in this work, the authors did not define a new element with different shape functions and geometry, and they used the sub-structuring capability of NASTRAN FE software to group a large number of conventional elements to be considered as an individual element. On one side, this methodology still needs the discretization step, and hence, the hassle of meshing still exists; on the other side, it is not limited to special geometries and can be used in analysis of structures with complex shapes. Many studies, especially in the analysis of large or complex industrial components or structures, have reported the use of this type of superelements [8-15].

For structures with revolving geometries, Ahmadian et al. [16] first introduced a new cylindrical superelement which can be applied in structural analysis of laminated hollow cylinders. This element was later modified by Taghvaeipour et al. [17] to be used in structural and modal analysis of thick hollow cylinders made of functionally graded materials (FGM); the results were compatible with the ones obtained by the conventional elements. In an industrial application, Pourhamid et al. [18] incorporated the cylindrical superelement for thermo-mechanical analysis of a functionally graded cylinder-piston with an internal pressure. Recently, Fatan et al. [19] modified this superelement to conduct vibration analysis of FGM rings. The same concept helped other researchers to develop the spherical and tapered versions of superelement to be used in mechanical analysis of revolving geometries, and structural analysis of components such as biologic cells, nano bearings, pressure vessels, fullerene, and etc. [20, 21, 22]. In a recent study, Shamloofard and Movahhedy [23] extended the tapered and spherical superelements to be used in thermo-mechanical analysis as well.

The shell structures have many applications in engineering design problems due to their advantages, which is superior to others. Some of the advantages are: high efficiency to handle a variety of loads, structural stability, strength to weight ratio, stiffness, and etc. Therefore, it is frequently used in the design of mechanical components such as pipes, turbine blades, pressure vessels, liquid retaining cylindrical shells, and aircraft structures. However, due to the presence of curvature, the analysis of a shell structure is more complex and cumbersome.

Since now, many researches targeted analytical and numerical analysis of shell structures in different conditions. Soleimani et al [24] has introduced a new cylindrical shell element by using modified couple stress theory. This new cylindrical shell element was developed to investigate the structural behavior of nanotubes. Torabi and Ansari [25] developed a new quadratic isoparametric superelement to analyze the vibration of FG circular shells. To show the accuracy and efficiency of the proposed superelement, different comparative studies were presented. Recently, a new shell superelement to study linear/nonlinear static analysis of spherical structures was presented by Shamloofard et al. [26]. The governing equations of spherical shells are derived based on the first-order shear deformation theory and considering large deformations. In this study, developing a new shell cylindrical superelement based on the classical shell theory is targeted. The geometry of this element is a hollow cylindrical shell, which one element can model the entire shell cylinder through the angular direction. This element can be used in mechanical analysis of cylindrical shell structures, such as thin-walled tubes and pressure vessels. As case studies, two classical problems in mechanical analysis of shell structures are solved, and the results are compared with the ones obtained analytically in the literature, and the result of shell elements which is conducted in a commercial software package.

2 Element Definition

2.1 Geometry and Coordinates

Generally, shell structures are divided into two types: thin- and thick-walled. The proposed shell superelement targets thin shells with a cylindrical geometry. The element has mid-surface radius of R, the thickness of t and the length of $2L$. The word "thin-walled" means, that t/R (wall thickness t to the mid-surface radius R ratio) is larger than 0.001 and less than 0.05 [27]. Moreover, the thickness t is considered constant all over the element. The coordinate system is chosen to be cylindrical and located at the center of the element. The nodes are distributed uniformly on the mid-surface at the two ends of element. Geometrical properties, coordinates, and nodes are shown in Figure (1). For convenience in calculation of the stiffness, mass, and force matrices, a natural coordinate system is defined [16]. This coordinate system has two components ξ and which are related to the axial z and angular components α, namely

$$\begin{gathered} \gamma = \frac{\alpha}{\pi} - 1, \quad \xi = \frac{z}{L} \\ 0 \le \alpha \le 2\pi, \quad -L \le z \le L \quad \rightarrow \quad -1 \le \xi, \gamma \le 1 \end{gathered} \tag{1}$$

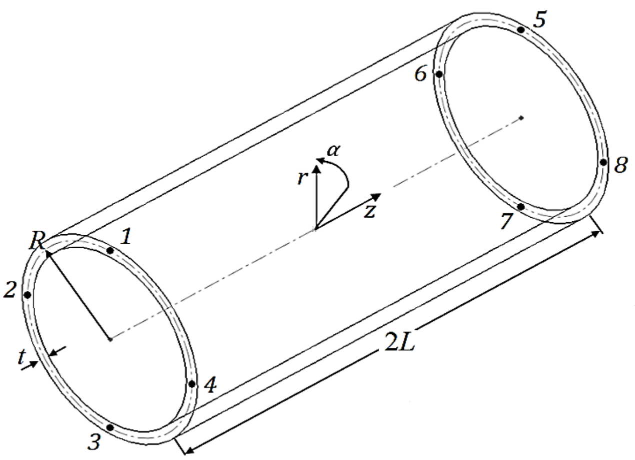

Figure 1 The shell superelement

2.2 The Shape Functions

The proposed shell element is defined based on the classical shell theory. In this theory it is assumed that the radial displacement component is independent of the radial coordinate [28]. Accordingly, the displacements in an arbitrary point of the shell are defined as [27]

$$\begin{aligned} w &= w^0 \\ v &= v^0 + (r - R)\beta_\alpha \\ u &= u^0 + (r - R)\beta_z \end{aligned} \tag{2}$$

Where w, v, and u are the radial, tangential and axial displacements, respectively, and w^0, v^0 and u^0 are the displacement components at the mid surface of the shell. Also, β_α and β_z are rotations in the tangential and axial directions, respectively. Due to Eqs. (2), v and u are dependent on the radial coordinate r, and w is independent of it. The rotations are also defined as [27]

$$\begin{aligned} \beta_\alpha &= \frac{v^0}{R} - \frac{1}{R}\frac{\partial w}{\partial \alpha} \\ \beta_z &= -\frac{\partial w}{\partial z} \end{aligned} \tag{3}$$

Since the rotations are functions of derivatives of w, the corresponding shape functions should be C^1-continous. However, other components of displacement vector are needed to be C^0-continuous [29, 30]. Therefore, the displacement vector at a point on the mid surface can be defined as

$$\mathbf{u} = \begin{bmatrix} w & \dfrac{\partial w}{\partial r} & \dfrac{\partial w}{\partial \alpha} & \dfrac{\partial^2 w}{\partial r \partial \alpha} & v^0 & u^0 \end{bmatrix}^T \tag{4}$$

In this superelement, the shape functions are defined as a combination of trigonometric and polynomial functions. Based on the foregoing discussion, the element needs 8×4 C^1-continuous and 8×2 C^0-continuous shape functions. Hence, the approximation function for the radial displacement is written as [29, 30]

$$\begin{aligned} w(z,\alpha) = N_1 w_1 + N_1' \left.\frac{\partial w}{\partial z}\right|_1 + N_1'' \left.\frac{\partial w}{\partial \alpha}\right|_1 + N_1''' \left.\frac{\partial^2 w}{\partial \alpha \partial z}\right|_1 + \ldots \\ N_8 w_8 + N_8' \left.\frac{\partial w}{\partial z}\right|_8 + N_8'' \left.\frac{\partial w}{\partial \alpha}\right|_8 + N_8''' \left.\frac{\partial^2 w}{\partial \alpha \partial z}\right|_8 \end{aligned} \tag{5}$$

Where N_i, N_i', N_i'', and $N_i'''$are C^1-continuous shape functions that are presented in the appendix A. Moreover, the tangential and axial displacements at the mid surface of the element are approximated as

$$\begin{aligned} v^0(z,\alpha) &= M_1 v_1^0 + M_2 v_2^0 + \ldots + M_8 v_8^0 \\ u^0(z,\alpha) &= M_1 u_1^0 + M_2 u_2^0 + \ldots + M_8 u_8^0 \end{aligned} \tag{6}$$

Where coefficients M_i are C^0-contiuous shape functions, given in the appendix A, and v_i^0 and u_i^0 are tangential and axial displacements at the nodes, respectively. As a result, this element has 32 + 8 = 40 distinct shape functions. By invoking to the FEM notation, the vector **u** in Eqs. (4) can be obtained by the following matrix relationship [16]

$$\{\mathbf{u}\} = [\mathbf{N}]\{\mathbf{q}\} \tag{7}$$

Where [**N**] is the matrix of shape functions and is defined below

$$[\mathbf{N}]=\begin{bmatrix} N_1 & 0 & 0 & 0 & 0 & 0 & & N_8 & 0 & 0 & 0 & 0 & 0 \\ 0 & N_1' & 0 & 0 & 0 & 0 & & 0 & N_8' & 0 & 0 & 0 & 0 \\ 0 & 0 & N_1'' & 0 & 0 & 0 & \cdots & 0 & 0 & N_8'' & 0 & 0 & 0 \\ 0 & 0 & 0 & N_1''' & 0 & 0 & & 0 & 0 & 0 & N_8''' & 0 & 0 \\ 0 & 0 & 0 & 0 & M_1 & 0 & & 0 & 0 & 0 & 0 & M_8 & 0 \\ 0 & 0 & 0 & 0 & 0 & M_1 & & 0 & 0 & 0 & 0 & 0 & M_8 \end{bmatrix}_{6\times 48} \tag{8}$$

And finally, the nodal displacement vector $\{\mathbf{q}\}$ is defined as following

$$\{\mathbf{q}\}=\begin{bmatrix} w_1 & \dfrac{\partial w_1}{\partial z} & \dfrac{\partial w_1}{\partial \alpha} & \dfrac{\partial^2 w_1}{\partial \alpha \partial z} & v_1^0 & u_1^0 & \cdots & w_8 & \dfrac{\partial w_8}{\partial z} & \dfrac{\partial w_8}{\partial \alpha} & \dfrac{\partial^2 w_8}{\partial \alpha \partial z} & v_8^0 & u_8^0 \end{bmatrix}_{1\times 48}^{T} \tag{9}$$

3 Stiffness and Force Matrices

3.1 Kinematic relations

In the classical shell theory, the shear strains $\gamma_{r\alpha}$ and γ_{zr} and the radial strain ε_{rr} are neglected [28]. The remained strains are considered functions of strains at the mid surface and curvatures, namely [31]

$$\begin{aligned} \varepsilon_z &= \varepsilon_z^0 + (r-R)\chi_z \\ \varepsilon_\alpha &= \varepsilon_\alpha^0 + (r-R)\chi_\alpha \\ \gamma_{\alpha z} &= \gamma_{\alpha z}^0 + 2(r-R)\chi_{\alpha z} \end{aligned} \tag{10}$$

Where $\varepsilon^0{}_z$, $\varepsilon^0{}_\alpha$, and $\gamma^0{}_{\alpha z}$ are strains at the mid surface which are functions of mid surface displacements

$$\varepsilon_z^0 = \frac{\partial u^0}{\partial z}, \qquad \varepsilon_\alpha^0 = \frac{1}{R}\frac{\partial v^0}{\partial \alpha} + \frac{w}{R}, \qquad \gamma_{\alpha z}^0 = \frac{1}{R}\frac{\partial u^0}{\partial \alpha} + \frac{\partial v^0}{\partial z} \tag{11}$$

And also, χ_z, χ_α, and $\chi_{\alpha z}$ are defined as the curvatures of shell which are defined below

$$\begin{aligned} \chi_z &= \frac{\partial \beta_z}{\partial z} = -\frac{\partial^2 w}{\partial z^2} \\ \chi_\alpha &= \frac{1}{R}\frac{\partial \beta_\alpha}{\partial \alpha} = \frac{1}{R}\frac{\partial}{\partial \alpha}\left(\frac{v^0}{R} - \frac{1}{R}\frac{\partial w}{\partial \alpha}\right) \\ \chi_{\alpha z} &= \frac{\partial \beta_\alpha}{\partial z} + \frac{1}{R}\frac{\partial \beta_z}{\partial \alpha} = \frac{\partial}{\partial z}\left(\frac{v^0}{R} - \frac{1}{R}\frac{\partial w}{\partial \alpha}\right) - \frac{1}{R}\frac{\partial}{\partial \alpha}\frac{\partial w}{\partial z} = \frac{1}{R}\frac{\partial}{\partial z}\left(v^0 - 2\frac{\partial w}{\partial \alpha}\right) \end{aligned} \tag{12}$$

3.2 Stress-strain relations

The three non-zero stress components of the element are related to the strains with the constitutive law of [31]

$$\begin{Bmatrix} \sigma_z \\ \sigma_\alpha \\ \tau_{\alpha z} \end{Bmatrix} = \begin{bmatrix} Q_{11} & Q_{12} & Q_{16} \\ Q_{12} & Q_{22} & Q_{26} \\ Q_{16} & Q_{26} & Q_{66} \end{bmatrix} \begin{Bmatrix} \varepsilon_z \\ \varepsilon_\alpha \\ \gamma_{\alpha z} \end{Bmatrix} = [\mathbf{Q}] \begin{Bmatrix} \varepsilon_z \\ \varepsilon_\alpha \\ \gamma_{\alpha z} \end{Bmatrix} \tag{13}$$

The matrix [**Q**] is called *the mechanical properties matrix* and its components for an isotropic material equals

$$Q_{11} = Q_{22} = \frac{E}{1-\nu^2}, \qquad Q_{12} = \frac{\nu E}{1-\nu^2}, \qquad Q_{66} = \frac{E}{2(1+\nu)} = G, \qquad Q_{16} = Q_{26} = 0 \tag{14}$$

Where E is the modulus of elasticity, G is the shear modulus, and ν is the Poisson ratio. By adding the thermal effects to the relations of Eqs. (11), the strain vector can be defined as

$$\begin{Bmatrix} \varepsilon_z \\ \varepsilon_\alpha \\ \gamma_{\alpha z} \end{Bmatrix} \begin{Bmatrix} \varepsilon_z^0 + (r-R)\chi_z - \alpha_e \Delta T \\ \varepsilon_\alpha^0 + (r-R)\chi_\alpha - \alpha_e \Delta T \\ \gamma_{\alpha z}^0 + 2(r-R)\chi_{\alpha z} - 2\alpha_e \Delta T \end{Bmatrix} \tag{15}$$

In which α_e is the thermal expansion coefficient and ΔT is the temperature difference of the shell from the reference temperature T_0. The strain-displacement and curvature-displacement relations, Eqs. (11) and (12) respectively, can be cast in a matrix form as

$$\{\boldsymbol{\varepsilon}\} = \{\varepsilon_z^0 \quad \varepsilon_\alpha^0 \quad \gamma_{\alpha z}^0 \quad \chi_z \quad \chi_\alpha \quad \chi_{\alpha z}\}^T = [\mathbf{L}]\{\mathbf{u}\} \tag{16}$$

In which [**L**] is an operator matrix which is given in the appendix A. After substitution of Eqs. (7) into Eqs. (16) it yields

$$\{\boldsymbol{\varepsilon}\} = [\mathbf{L}]\{\mathbf{u}\} = [\mathbf{L}][\mathbf{N}]\{\mathbf{q}\} = [\mathbf{B}]\{\mathbf{q}\} \tag{17}$$

Where

$$[\mathbf{B}]_{6\times 48} = [\mathbf{L}]_{6\times 6} \times [\mathbf{N}]_{6\times 48} \tag{18}$$

3.3 Element stiffness matrix and force vectors

In FEM, the final form of the system of equations between the displacement and force vectors of element is expressed as

$$[\mathbf{K}_\mathbf{u}]^{(e)} \{\mathbf{q}\}^{(e)} = \{\mathbf{f}\}^{(e)} \tag{19}$$

Where $[\mathbf{K}_\mathbf{u}]^{(e)}$ is called the stiffness matrix of element, and here, it is derived from the Ritz method and in terms of the natural coordinates [29]

$$[\mathbf{K}_\mathbf{u}]^{(e)} = RL\pi \int_{-1}^{1}\int_{-1}^{1} [\mathbf{B}]^T [\mathbf{D}_\mathbf{e}][\mathbf{B}]\, d\xi\, d\gamma \tag{20}$$

Also, [$\mathbf{D}_\mathbf{e}$] is the material properties matrix which is defined as [31]

$$[\mathbf{D_e}] = \begin{bmatrix} A_{11} & A_{12} & 0 & 0 & 0 & 0 \\ A_{12} & A_{22} & 0 & 0 & 0 & 0 \\ 0 & 0 & A_{66} & 0 & 0 & 0 \\ 0 & 0 & 0 & D_{11} & D_{12} & 0 \\ 0 & 0 & 0 & D_{12} & D_{22} & 0 \\ 0 & 0 & 0 & 0 & 0 & D_{66} \end{bmatrix} \tag{21}$$

$$A_{11} = A_{22} = \frac{Et}{1-\nu^2}, \qquad A_{12} = \frac{\nu Et}{1-\nu^2}, \qquad A_{66} = \frac{Et}{2(1+\nu)} = Gt$$

$$D_{11} = D_{22} = \frac{Et^3}{12(1-\nu^2)}, \qquad D_{12} = \frac{\nu Et^3}{12(1-\nu^2)}, \qquad D_{66} = \frac{Et^3}{24(1+\nu)} = \frac{Gt^3}{12}$$

The force vector $\{\mathbf{f}\}^{(e)}$ in Eqs. (19) contains the external mechanical and thermal loads on the element [29], namely

$$\{\mathbf{f}\}^{(e)} = \{\mathbf{f_T}\}^{(e)} + \{\mathbf{f_{bf}}\}^{(e)} + \{\mathbf{f_{df}}\}^{(e)} + \{\mathbf{f_{cf}}\}^{(e)} \tag{22}$$

where in the foregoing case study, the right hand vectors are defined below:

- Thermal loads vector

$$\begin{gathered} \{\mathbf{f_T}\}^{(e)} = RL\pi \int_{-1}^{1}\int_{-1}^{1} [\mathbf{B}]^T \{\mathbf{S_r}^{\mathbf{T}}\} d\xi\, d\gamma \\ \{\mathbf{S_r}^{\mathbf{T}}\} = \{N_z^T \quad N_\alpha^T \quad 0 \quad M_z^T \quad M_\alpha^T \quad 0\} \end{gathered} \tag{23}$$

in which $\{\mathbf{S_r}^{\mathbf{T}}\}$is the force and momentum resultant vector that is produced due to a temperature difference, and its components are defined below

$$\begin{Bmatrix} N_z^T \\ N_\alpha^T \end{Bmatrix} = \int_{R-\frac{t}{2}}^{R+\frac{t}{2}} \begin{Bmatrix} Q_{11} + Q_{12} \\ Q_{12} + Q_{22} \end{Bmatrix} \alpha_e \Delta T dr \tag{24}$$

$$\begin{Bmatrix} M_z^T \\ M_\alpha^T \end{Bmatrix} = \int_{R-\frac{t}{2}}^{R+\frac{t}{2}} \begin{Bmatrix} Q_{11} + Q_{12} \\ Q_{12} + Q_{22} \end{Bmatrix} (r-R) \alpha_e \Delta T dr \tag{25}$$

- The body force vector

$$\{\mathbf{f_{bf}}\}^{(e)} = \int_{V^{(e)}} [\mathbf{N_u}]^T \{\mathbf{x_i}\} dV \tag{26}$$

- The distributed force vector

$$\{\mathbf{f_{df}}\}^{(e)} = \int_{A^{(e)}} [\mathbf{N_u}]^T \{\mathbf{f_d}\} dA \tag{27}$$

- The concentrated force vector

$$\{\mathbf{f_{cf}}\}^{(e)} = \left[F_r^1 \quad M_z^1 \quad M_\alpha^1 \quad M_{\alpha z}^1 \quad F_\alpha^1 \quad F_z^1 \quad \cdots \quad F_r^8 \quad M_z^8 \quad M_\alpha^8 \quad M_{\alpha z}^8 \quad F_\alpha^8 \quad F_z^8\right]^T \tag{28}$$

4 Results and discussion

To validate the defined element, two classical shell structure problems are considered and the results are compared with the analytical solutions available in the literature and also with the results which is obtained by means of shell elements in a commercial software package.

4.1 Problem I

Consider a storage tank standing on the ground and filled with the water. The tank is open on top and water has a free surface. Therefore, the pressure varies linearly from the top to bottom of the tank. The tank is made of cement by the order of C25 with the elasticity modulus of E = 20GPa and Poisson's ratio of $\nu = 0.2$. Also, the specific weight of the water is γ = 10 kN/m^3. The tank dimensions are depicted in Figure (2). The radial displacements of the tank through the length are desired.

4.1.1 The Result

By resorting to only five shell superelements, the deformations of the tank undergoing the water pressure are obtained, and the results are compared with the analytical solutions presented in [32]. Also, by resorting to a commercial software package, the results are compared with those obtained by 2000 shell elements. Figure (3) depicts the radial displacement curves obtained by superelements, the analytical method, and shell elements.
As it is apparent, with only five elements the radial deformation curve is properly matched with the analytical one and 2000 shell elements. In the same Figure, the results for 10 superelements are also presented. With the higher number of elements, the result is almost converged to the analytical one, however, according to the obtained maximum relative errors which are reported in the Table (1); five superelements adequately conduct the deformation analysis. superelement, an analytical method presented in [32], and shell elements. By having the nodal displacements at hand, the stress components, at any location, can be derived. Figure (4) shows the tangential stress profile with respect to the height of the cylinder which is computed by 5 and 10 superelements. In this Figure, the stress result which was obtained analytically in [32], and numerically with 2000 shell elements are also depicted. Apparently, the superelement method is also proved to be efficient in the calculation of stress result.
In Table (1), the effect of number of superelements on the accuracy of the results is presented.

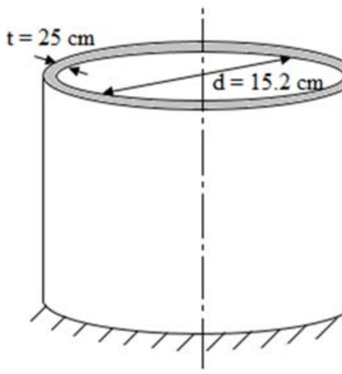

Figure 2 The storage tank of problem I

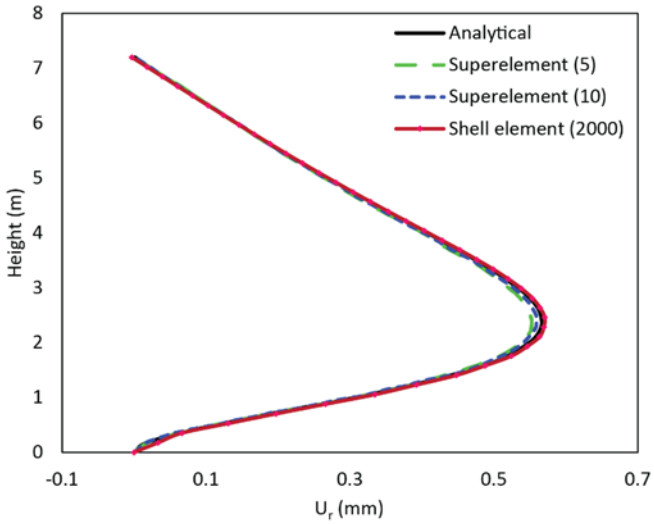

Figure 3 The radial displacement curve of the storage tank with respect to the height obtained by the

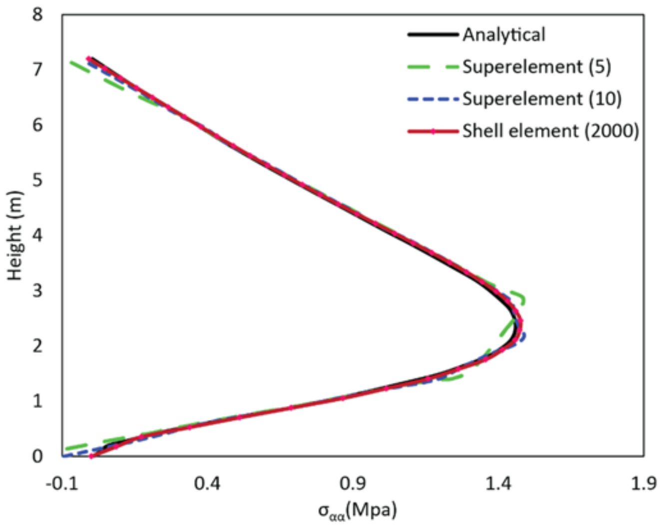

Figure 4 The tangential stress profile of the storage tank through the height obtained by the superelement, an analytical method presented in [32], and shell elements

Table 1 Maximum relative errors of radial displacements and tangential stresses obtained with different number of superlements.

Element Type	Number of Elements	Maximum Relative Error of u_r (%)	Maximum Relative Error of $\sigma_{\alpha\alpha}$ (%)
Superelement	5	2.32	3.31
Superelement	10	1.18	2.65
Superelement	15	0.66	1.22
Superelement	20	0.19	0.41
Shell element	1000	1.28	1.68
Shell element	2000	0.95	1.46

4.2 Problem II

In this example, a thin cylindrical tank filled with the water is placed horizontally on the end supports (Figure (5)). The tank ends are simply supported so that the radial and tangential displacements vanish. The tank has a radius of R = 1m, thickness of t = 3mm and the length of L_c = 5m, and it is made of stainless steel with elasticity modulus of E = 200GPa and Poisson ratio of ν = 0.28.

Here, the effect of weight of water is neglected and only a distributed pressure inside the tank is considered. The boundary conditions at both ends are defined as following

$$\begin{aligned} z = 0 &\rightarrow u_\alpha = u_r = 0 \\ z = L_c &\rightarrow u_\alpha = u_r = 0 \end{aligned} \tag{29}$$

It is assumed that the distributed load is asymmetric through the angular direction, namely

$$P = \gamma_w R \left(1 + \cos(\theta)\right) \tag{30}$$

The analytical solutions of this problem are presented in [33] which, beside the results of shell elements in a commercial software package, will be used as a verification of the superelement method.

4.2.1 The Results

The problem is first solved by five and then by 10 superelements. The radial displacements at L = 2m with respect to angle θ are depicted in Figure (6). The analytical result which was presented in [33], and the ones which are obtained by 2400 shell elements are also depicted in Figure. 6. The corresponding tangential stress result is also plotted in Figure (7). The stress result is obtained based on the *recovery method*, which is thoroughly explained in [34]. Moreover, Figures (8) and (9) show the graphs of radial displacement and the tangential stress result at θ = 0 with respect to the length of cylinder, respectively. As it is obvious, the superelements can estimate the displacements and stresses properly, comparing with the analytical ones. Although the governing equations of the problem include the second derivative of the tangential displacement, the trigonometric shape functions of a superelement are properly estimate the results. Table (2) presents the maximum relative errors of the obtained radial displacements and tangential stresses calculated by different number of elements. As the stress result is derived from the nodal displacements, higher relative error is expected. From Figures (6), (7), (8) and (9) and the Table (2) it is apparent that even five superelements is enough to predict the deformation and stress results properly with almost 3% and 7% maximum relative error, respectively. However, if a better accuracy is needed, especially in stress analysis, more superelements is required. For example, as the Table (2) shows, by incorporating 10superelements the maximum relative error of the derived stress results drops to 2.65%.

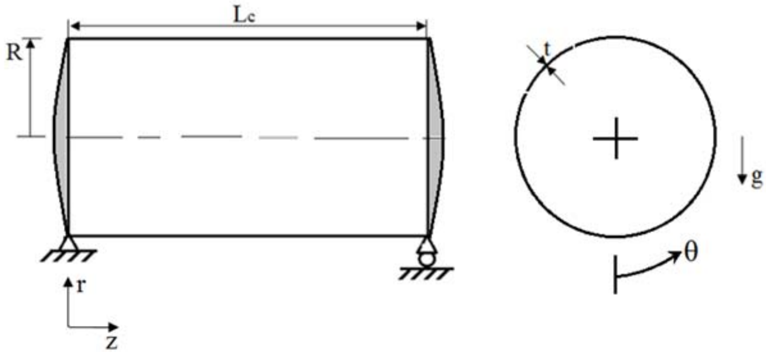

Figure 5 The cylindrical tank of problem II

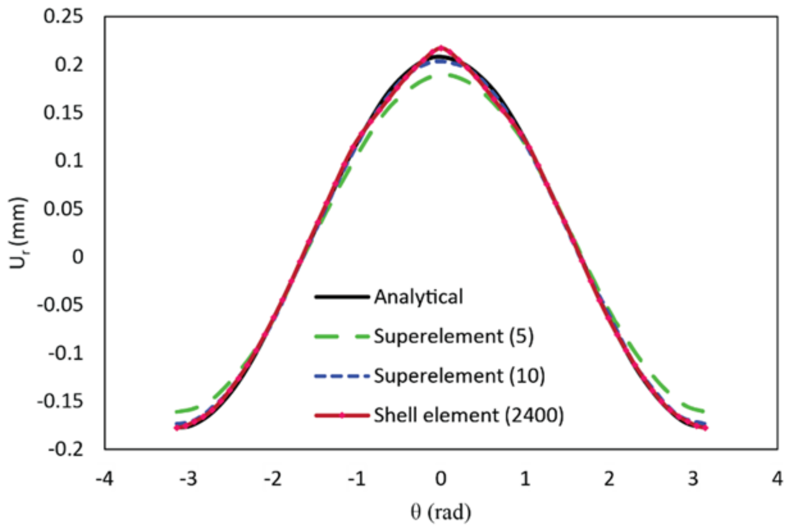

Figure 6 The radial displacement with respect to θ obtained by superelements, the analytical method presented in [33], and shell elements.

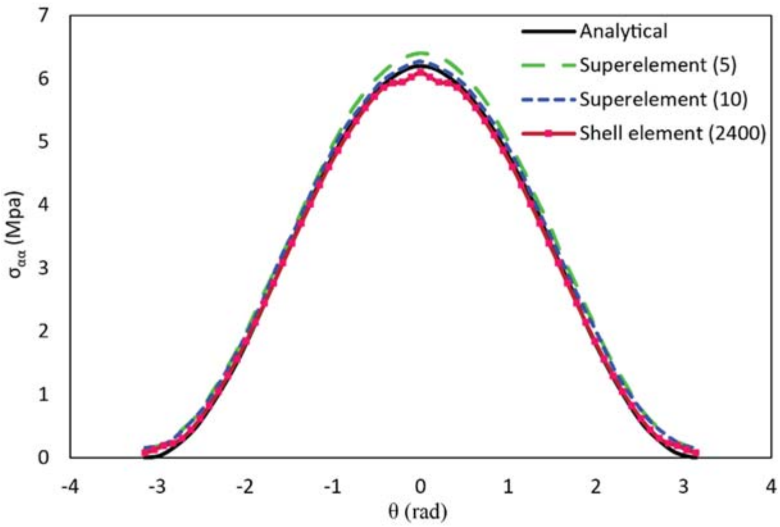

Figure 7 The tangential stress plot with respect to θ obtained by superelements, an analytical method presented in [33], and shell elements.

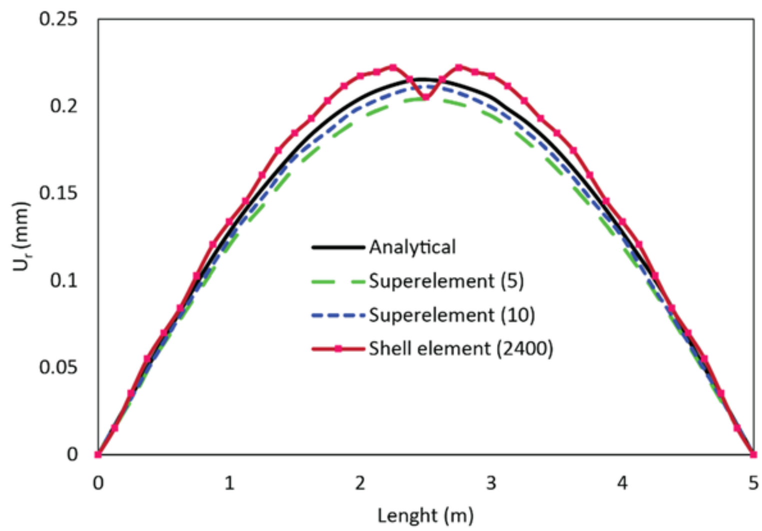

Figure 8 The radial displacement with respect to the length obtained by superelements, an analytical method presented in [33], and shell elements.

Table 2 Maximum relative errors of radial displacements and tangential stresses obtained with different number of superlements.

Element Type	Number of Elements	Maximum Relative Error of u_r (%)	Maximum Relative Error of $\sigma_{\alpha\alpha}$ (%)
Superelement	5	2.32	3.31
Superelement	10	1.18	2.65
Superelement	15	0.66	1.22
Superelement	20	0.19	0.41
Shell element	2400	4.38	4.13

Finally, the tangential stress contour of the cylindrical shell along the z and θ directions which is obtained by 10 superelements are displayed in the Figure (10).

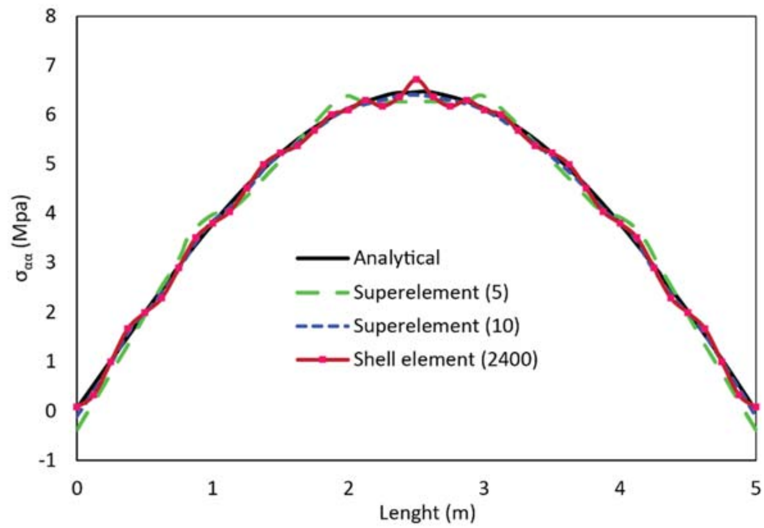

Figure 9 The tangential stress plot with respect to the length obtained by superelements the analytical method presented in [33], and shell elements.

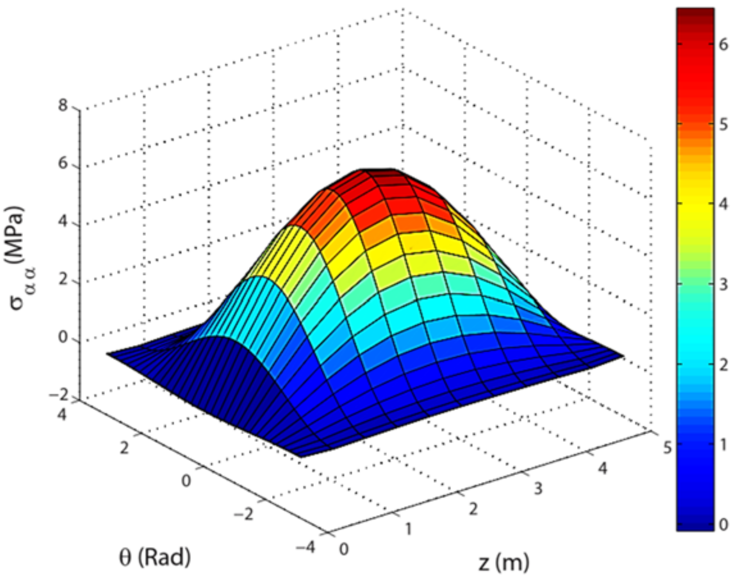

Figure 10 The tangential stress plot of the cylindrical shell through the z and θ directions obtained by 10 superelements.

5 Conclusions

In this paper, the development of a novel cylindrical shell element is targeted. This element provides high speed and accuracy in the mechanical analysis of cylindrical shell structures. The shape functions of this element are a combination of polynomial and trigonometric functions which provide high accuracy in the estimation of nodal displacements and stress components in problems with asymmetric loadings. This was examined by a classical case study in which an asymmetric loading was applied. Although this type of elements is constrained by a certain geometry, it can be effectively incorporated in complex problems such as nonlinear analysis of structures made of complex materials, like composites or functionally graded materials.

References

[1] Koko T.S., "Super Finite Elements for Nonlinear Static and Dynamic Analysis of Stiffened Plate Structures", Ph.D. Thesis, University of British Columbia, Vancouver, Canada, (1990).

[2] Koko, T.S., and and Olson, M.D., "Vibration Analysis of Stiffened Plates by Superelements", J. Sound Vib., Vol. 158, pp. 149-167, (1992).

[3] Jiang, J., and Olson, M.D., "Vibration Analysis of Orthogonally Stiffened Cylindrical Shells using Super Finite Elements", J. Sound Vib., Vol. 173, pp. 73-83, (1994).

[4] Jiang, J., and Olson, M.D., "Nonlinear Analysis of Orthogonally Stiffened Cylindrical Shells by a Superelement Approach", Finite Elem. Anal. Des., Vol. 18, pp. 99-110, (1994).

[5] Ahmadian, M.T., and Zanganeh, M.S., "Vibration Analysis of Orthotropic Rectangular Plates using Superelements", Comput. Methods Appl. Mech. Eng., Vol. 191, pp. 2069-2075, (2002).

[6] Ahmadian, M.T., and Zanganeh, M.S. "Application of Superelements to Free Vibration Analysis of Laminated Stiffened Plates", J. Sound Vib., Vol. 259, pp. 1243-1252, (2003).

[7] Kuntjoro, W., Abdul Jalil AMH, Mahmun J., "Wing Structure Analysis using Superelement", Procedia Engineering, Vol. 41, pp. 1600-1606, (2012).

[8] Tkachev, V.V., "The use of Superelement Approach for the Mathematical Simulation of Reactor Structure Dynamic Behavior", Nuclear Engineering and Design, Vol. 196, pp. 101-104, (2000).

[9] Ju, F., and Choo, Y.S., "Superelement Approach to Cable Passing through Multiple Pulleys", Int. J. Solids Struct., Vol. 42, pp. 3533-3547, (2005).

[10] He, Y.J., Zhou, X.H., and Hou, P.F., "Combined Method of Super Element and Substructure for Analysis of ILTDBS Reticulated Mega-structure with Single-layer Latticed Shell Substructures", Finite Element in Analysis and Design, Vol. 46, pp. 563-570, (2010).

[11] Tahilramani, D.R., and Hitchins, J., "Application of Model Reduction Techniques within Cummins Inc.", Proceedings of the ASME 2014 Internal Combustion Engine Division Fall Technical Conference, Columbus, USA, pp. 19-22, (2014).

[12] Danielczyk, P., “Parametric Optimization with the use of Numerically Efficient Finite Element Models”, Advances in Mechanical Engineering, Vol. 11, pp. 1-12, (2015).

[13] Persson, P., Persson, K., and Sandberg, G., “Reduced order Modeling of Liquid-filled Pipe Systems”, Journal of Fluids and Structures, Vol. 61, pp. 205-217, (2016).

[14] Lu, C., Yang, W., Zheng, H., Liang, J., and Fu, G., “The Application of Superelement Modeling Method in Vehicle Body Dynamics Simulation”, SAE Technical Paper, doi: 2016-01-8050, (2016).

[15] Semenov, S., Nikhamkin, M., Sazhenkov, N., Semenov, I., and Mekhonoshin, G., “Simulation of Rotor System Vibrations using Experimentally Verified Super Elements”, Proceedings of the ASME International Mechanical Engineering Congress and Exposition (IMECE2016), Phoenix, Arizona, USA, pp. 11-17, (2016).

[16] Ahmadian, M.T., and Bonakdar, M., “A New Cylindrical Element Formulation and its Application to Structural Analysis of Laminated Hollow Cylinders”, Finite Elem. Anal. Des., Vol. 44, pp. 617-630, (2008).

[17] Taghvaeipour, A., Bonakdar, M., and Ahmadian, M.T., “Application of a New Cylindrical Element Formulation in Finite Element Structural Analysis of FGM Hollow Cylinders”, Finite Element Analysis Design, Vol. 50, pp, 1-7, (2012).

[18] Pourhamid, R., Ahmadian, M.T., Mahdavy Moghaddam, H., and Mohammadzadeh, A.R., “Mechanical Analysis of a Functionally Graded Cylinder-piston under Internal Pressure Due to a Combustion Engine using a Cylindrical Super Element and Considering Thermal Loading”, Scientia Iranica B, Vol. 22, pp. 493-503, (2015).

[19] Fatan A.R., and Ahmadian, M.T., “Vibration Analysis of FGM Rings using a Newly Designed Cylindrical Superelement”, Scientia Iranica B, Vol. 25, pp. 1179-1188, (2018).

[20] Nasiri Sarvi, M., and Ahmadian, M.T., “Design and Implementation of a New Spherical Superelement in Structural Analysis”, Appl. Math. Comput., Vol. 218, pp. 7546-7561, (2012).

[21] Nasiri Sarvi, M., and Ahmadian, M.T., “Static and Vibrational Analysis of Fullerene using a Newly Designed Spherical Element”, Scientia Iranica B, Vol. 19, pp. 1316-1323, (2012).

[22] Ahmadian, M.T., Movahhedy, M.R., and Rezaei, M.M., “Design and Application of a New Tapered Superelement for Analysis of Revolving Geometries”, Finite Elem. Anal. Des., Vol. 47, pp. 1242-1252, (2011).

[23] Shamloofard, M., and Movahhedy, M.R., “Development of Thermo-elastic Tapered and Spherical Superelements”, Applied Mathematics and Computation, Vol. 265, pp. 380-399, (2015).

[24] Soleimani, I., Tadi Beni, Y., and Mehralian, F., “A New Size-Dependent Cylindrical Shell Element Based on Modified Couple Stress Theory”, Adv. Appl. Math. Mech., Vol. 10, pp. 819-844, (2017).

[25] Torabi, J., and Ansari, R., “A Higher-order Isoparametric Superelement for Free Vibration Analysis of Functionally Graded Shells of Revolution”, Thin-Walled Structures, Vol. 133, pp. 169-179, (2018).

[26] Shamloofard, M., Hosseinzadeh, A., and Movahhedy, M.R., "Development of a Shell Superelement for Large Deformation and Free Vibration Analysis of Composite Spherical Shells", Engineering with Computers, (2020). https://doi.org/10.1007/s00366-020-01015-w.

[27] Venstel, E., and Krouthammer, T., "*Thin Plates and Shells, Theory, Analysis, and Applications*", First Ed, Marcel Dekker, New York, USA, (2001).

[28] Reddy, J. N., and Lio, C. F., "A Higher-order Shear Deformation Theory of Laminated Elastic Shells", International Journal of Engineering Science, Vol. 23, pp. 319-330, (1985).

[29] Eslami, M.R., "*Finite Elements Methods in Mechanics*", First Ed, Springer, Switzerland, (2014).

[30] Rao, S.S., "*The Finite Element Method in Engineering*", Fifth Ed, Butterworth-Heinemann, United Kingdom, (2011).

[31] Jin, G., Ye, T., Chen, Y., Su, Z., and Yan, Y., "An Exact Solution for the Free Vibration Analysis of Laminated Composite Cylindrical Shells with General Elastic Boundary Conditions", Composite Structures, Vol. 106, pp. 114-127, (2013).

[32] Blaauwendraad, J., and Hoefakker, J.H., "*Structural Shell Analysis (Understanding and Application)*", First Ed, Springer, New York, USA, (2014).

[33] Timoshenko, S., and Woinowski-Krieger, S., "*Theory of Plate and Shells*", Second Ed, McGraw-Hill, New York, USA, (1959).

[34] Felippa, C., "Introduction to Finite Element Methods (ASEN 5007)", Lecture Notes, Department of Aerospace Engineering Sciences, University of Colorado at Boulder, USA, http://www.colorado.edu/engineering/CAS/courses/IFEM.

Nomenclature

A_{ij}, D_{ij}	Material properties matrix elements
E	Modulus of elasticity
F^{i}_{α}	Tangential concentrated force
F^{i}_{z}	Axial concentrated force
G	Shear Modulus
L	Half-length of element
M^{T}_{z}	Axial momentum resultant of temperature difference
M^{T}_{α}	Tangential momentum resultant of temperature difference
N^{T}_{z}	Axial force resultant of temperature difference
N^{T}_{α}	Tangential force resultant of temperature difference
M^{i}_{z}	Axial concentrated momentum resultant
M^{i}_{α}	Tangential concentrated momentum resultant
N^{i}_{z}	Axial concentrated force resultant

N^i_α	Tangential concentrated force resultant
Q_{ij}	Mechanical properties matrix elements
r	Radial Coordinate of element
R	Element radius
ΔT	Temperature difference
u	Total radial displacement
u^0	Radial displacement of element mid-surface
v	Total tangential displacement
v^0	Tangential displacement of element mid-surface
w	Total Axial displacement
w^0	Axial displacement of element mid-surface
z	Axial Coordinate of element
Greek symbols	
α	Tangential Coordinate
α_e	Thermal expansion coefficient
β_α	Tangential rotation of element
β_z	Axil rotation of element
γ	Tangential local coordinate
$\gamma_{\alpha z}$	Total shear strain
$\gamma^0_{\alpha z}$	shear strain of mid-surface
ε_α	Total tangential normal strain
ε^0_α	Tangential normal strain of mid-surface
ε_z	Total Axial normal strain
ε^0_z	Axial normal strain of mid-surface
ν	Poisson ratio
ξ	Axial local coordinate
σ_α	Tangential stress
σ_z	Axial stress
$\tau_{\alpha z}$	Shear stress
χ_α	Tangential curvature
χ_z	Axial curvature
$\chi_{\alpha z}$	Transverse curvature

Appendix A

C^1-continuous shape functions

$$\begin{aligned}
N_{i,j} &= f_i(\xi) g_j(\gamma) \\
N'_{i,j} &= F_i(\xi) g_j(\gamma) \\
N''_{i,j} &= f_i(\xi) G_j(\gamma) \\
N'''_{i,j} &= F_i(\xi) G_j(\gamma) \\
i = 1, 2 \quad & j = 1, \ldots 4
\end{aligned} \tag{A1}$$

Where

$$\begin{cases}
f_1(\xi) = \frac{1}{4}\left(\xi^3 - 3\xi + 2\right) \\
f_2(\xi) = -\frac{1}{4}\left(\xi^3 - 3\xi - 2\right)
\end{cases}$$

$$\begin{cases}
F_1(\xi) = \frac{1}{4}\left(\xi^3 - \xi^2 - \xi + 1\right) \\
F_2(\xi) = \frac{1}{4}\left(\xi^3 + \xi^2 - \xi - 1\right)
\end{cases}$$

$$\begin{cases}
g_1(\gamma) = \frac{1}{8}\left(-3cos\ \pi\gamma + 2cos\ 2\pi\gamma - cos\ 3\pi\gamma + 2\right) \\
g_2(\gamma) = \frac{1}{8}\left(-3sin\ \pi\gamma - 2cos\ 2\pi\gamma + sin\ 3\pi\gamma + 2\right) \\
g_3(\gamma) = \frac{1}{8}\left(3cos\ \pi\gamma + 2cos\ 2\pi\gamma + cos\ 3\pi\gamma + 2\right) \\
g_4(\gamma) = \frac{1}{8}\left(3sin\ \pi\gamma - 2cos\ 2\pi\gamma - sin\ 3\pi\gamma + 2\right)
\end{cases}$$

$$\begin{cases}
G_1(\gamma) = \frac{1}{8\pi}\left(-sin\ \pi\gamma + sin\ 2\pi\gamma - sin\ 3\pi\gamma + \frac{1}{2}sin\ 4\pi\gamma\right) \\
G_2(\gamma) = \frac{1}{8\pi}\left(cos\ \pi\gamma - sin\ 2\pi\gamma - cos\ 3\pi\gamma + \frac{1}{2}sin\ 4\pi\gamma\right) \\
G_3(\gamma) = \frac{1}{8\pi}\left(sin\ \pi\gamma + sin\ 2\pi\gamma + sin\ 3\pi\gamma + \frac{1}{2}sin\ 4\pi\gamma\right) \\
G_4(\gamma) = \frac{1}{8\pi}\left(-cos\ \pi\gamma - sin\ 2\pi\gamma + cos\ 3\pi\gamma + \frac{1}{2}sin\ 4\pi\gamma\right)
\end{cases}$$

C^0-continuous shape functions:

$$
\begin{aligned}
&M_{i,j} = h_i(\xi) I_j(\gamma) \\
&i = 1,2 \quad j = 1,\dots 4
\end{aligned}
\tag{A2}
$$

Where:

$$
\begin{cases}
h_1(\xi) = \dfrac{1}{2}(1-\xi) \\
h_2(\xi) = \dfrac{1}{2}(1+\xi)
\end{cases}
$$

$$
\begin{cases}
I_1(\gamma) = \dfrac{1}{4}\left(1 - 2cos\ \pi\gamma + cos\ 2\pi\gamma\right) \\
I_2(\gamma) = \dfrac{1}{4}\left(1 - 2sin\ \pi\gamma - cos\ 2\pi\gamma\right) \\
I_3(\gamma) = \dfrac{1}{4}\left(1 + 2cos\ \pi\gamma + cos\ 2\pi\gamma\right) \\
I_4(\gamma) = \dfrac{1}{4}\left(1 + 2sin\ \pi\gamma - cos\ 2\pi\gamma\right)
\end{cases}
$$

The numbering of indexes i and j in Eqs. (A1) and Eqs. (A2) are according to Figure (A1). Operator matrix [**L**] is defined as:

$$
[\mathbf{L}] = \begin{bmatrix}
0 & 0 & 0 & 0 & 0 & \dfrac{\partial}{\partial z} \\
\dfrac{1}{R} & \dfrac{1}{R} & \dfrac{1}{R} & \dfrac{1}{R} & \dfrac{1}{R}\dfrac{\partial}{\partial \alpha} & 0 \\
0 & 0 & 0 & 0 & \dfrac{\partial}{\partial z} & \dfrac{1}{R}\dfrac{\partial}{\partial \alpha} \\
-\dfrac{\partial^2}{\partial z^2} & -\dfrac{\partial^2}{\partial z^2} & -\dfrac{\partial^2}{\partial z^2} & -\dfrac{\partial^2}{\partial z^2} & 0 & 0 \\
-\dfrac{1}{R^2}\dfrac{\partial^2}{\partial \alpha^2} & -\dfrac{1}{R^2}\dfrac{\partial^2}{\partial \alpha^2} & -\dfrac{1}{R^2}\dfrac{\partial^2}{\partial \alpha^2} & -\dfrac{1}{R^2}\dfrac{\partial^2}{\partial \alpha^2} & \dfrac{1}{R^2}\dfrac{\partial}{\partial \alpha} & 0 \\
-\dfrac{1}{R}\dfrac{\partial^2}{\partial \alpha \partial z} & -\dfrac{1}{R}\dfrac{\partial^2}{\partial \alpha \partial z} & -\dfrac{1}{R}\dfrac{\partial^2}{\partial \alpha \partial z} & -\dfrac{1}{R}\dfrac{\partial^2}{\partial \alpha \partial z} & \dfrac{1}{2R}\dfrac{\partial}{\partial z} & 0
\end{bmatrix}_{6\times 6}
$$